

Ultrasound-responsive gene-activated matrices (GAMs) for osteogenic gene therapy using matrix-assisted sonoporation (MAS)

N. Nomikou^{†1}, G.A. Feichtinger^{†*2,3}, S. Saha³, S. Nuernberger^{4,5}, P. Heime², H. Redl²,
A.P. McHale^{*6}

¹*Research Department of General Surgery, Division of Surgery & Interventional Science, Faculty of Medical Sciences, University College London, London, UK*

²*Ludwig Boltzmann Institute for Experimental and Clinical Traumatology, AUVA Research Centre, Austrian Cluster for Tissue Regeneration, European Institute of Excellence on Tissue Engineering and Regenerative Medicine Research (Expertissues EEIG), Vienna- Branch, Vienna, Austria*

³*Department of Oral Biology, School of Dentistry, University of Leeds, Leeds, UK*

⁴*Medical University of Vienna, Department of Traumatology, Vienna, Austria*

⁵*Bernhard Gottlieb University Clinic of Dentistry, Vienna, Austria*

⁶*School of Pharmacy and Pharmaceutical Sciences, University of Ulster, Coleraine, UK*

[†] *Both authors contributed equally to this study*

^{*}*Authors to whom correspondence should be addressed*

Corresponding authors:

Dr. Georg A. Feichtinger

Prof. Anthony P. McHale

Department of Oral Biology

School of Pharm. & Pharmaceut. Sciences

University of Leeds

University of Ulster

P: +44-11334-35569

P: +44-28-70124616

Fax: +44-1133436548

Email: g.feichtinger@leeds.ac.uk

Email: ap.mchale@ulster.ac.uk

Abstract: Gene-activated matrix (GAM)-based therapeutics for tissue regeneration are limited by efficacy, the lack of spatiotemporal control and availability of target cells, all of which impact negatively on their translation to the clinic. Here we describe an advanced ultrasound-responsive GAM containing target cells that facilitates matrix-assisted sonoporation (MAS) to induce osteogenic differentiation. Ultrasound-responsive GAMs consisting of fibrin/collagen hybrid-matrices containing microbubbles, bone morphogenetic protein BMP2/7 co-expression plasmids together with C2C12 cells were treated with ultrasound either *in vitro* or following parenteral intramuscular implantation *in vivo*. Using direct measurement for alkaline phosphatase activity, von Kossa staining and immuno-histochemical analysis for osteocalcin expression, MAS-stimulated osteogenic differentiation was confirmed in the GAMs *in vitro* 7 days after treatment with ultrasound. At day 30 post-treatment with ultrasound, ectopic osteogenic differentiation was confirmed *in vivo* using X-ray microcomputed tomography (μ CT) and histological analysis. Osteogenic differentiation was indicated by the presence of ectopic bone structures in all animals treated with MAS. In addition, bone volumes in this group were statistically greater than those in the control groups. This novel approach of incorporating a MAS capability into GAMs could be exploited to facilitate *ex vivo* gene transfer with subsequent surgical implantation or alternatively provide a minimally invasive means of stimulating *in situ* transgene delivery for osteoinductive gene-based therapies.

Key Words: Osteogenesis, gene, matrix, sonoporation, ultrasound, regeneration.

1. Introduction

Gene-activated matrices (GAMs) are smart biomaterials designed to deliver therapeutic genes *in vivo* in order to augment wound-healing by inducing a local niche of regeneration with appropriate transient differentiation cues produced by genetically modified precursor cells (Bonadio, 2000; Balmayor and van Griensven, 2015). Traditional GAMs usually consist of a natural biopolymer carrier matrix with the potential to support tissue regeneration as a scaffold, retain secreted factors in an extracellular matrix (ECM)-like microenvironment and provide therapeutic nucleic acids encoding a growth or differentiation factor that deliver the stimulus for tissue formation (Lu *et al.*, 2013; Tierney *et al.*, 2013). Whilst GAM systems have been reported that use viral gene transfer approaches (Balmayor and van Griensven 2015; Peterson *et al.*, 2009), it has been suggested that GAMs employing non-viral strategies using episomal elements such as DNA plasmids are preferable because they deliver transient expression and incorporate less risk (Yin *et al.*, 2014). Owing to their safety and low therapeutic cost profile, GAMs have been extensively investigated over the past 16 years. The breadth of their potential clinical applications range is indicated by numerous studies that have successfully demonstrated their experimental use in bone regeneration (Lu *et al.*, 2013), cartilage regeneration (Kayabashi *et al.*, 2013), osteochondral regeneration (Schillinger *et al.*, 2008), wound healing (Michlits *et al.*, 2007) and cardiac and neuro-regeneration (Gonzales *et al.*, 2006). Despite these exciting reports, very few GAM-based approaches have been clinically tested and this is due, at least in part, to the traditionally low gene delivery efficacies provided by non-viral gene transfer modalities (Ramamooth and Narvekar, 2015). The high doses of nucleic acid necessitated by low gene transfer efficacy and the resulting potential of transgene persistence or dispersion at off-target sites *in vivo*, has significantly impaired the development of this technology (Jafari *et al.*, 2012; Wang *et al.*, 2013). A clear un-met need therefore exists

in this area for approaches that can safely provide effective and controlled delivery of transgenes to target cells in 3D environments *in situ*.

Many approaches have been developed over the years to enhance gene transfer efficiencies in GAMs and some of these have yielded promising results (Tierney *et al.*, 2013; Wang *et al.*, 2015). However, the use of approaches that are unlicensed for human use or remain untested in 3D matrices hinders accelerated straightforward translation to the clinic (Yin *et al.*, 2014). In addition, the lack of *in situ* spatiotemporal control on gene transfer and expression in existing GAM designs provides another significant challenge to their widespread clinical use as a controlled regenerative modality (Tierney *et al.*, 2013).

Ultrasound-mediated, microbubble-enhanced gene delivery is a minimally invasive, physical gene transfer modality, which has been shown to promote intracellular delivery of nucleic acid *in vitro* and *in vivo* (Escoffre *et al.*, 2013). In addition, the use of ultrasound together with microbubbles to enhance cellular uptake of therapeutic agents has an excellent safety profile (Lammertink *et al.*, 2015). The above attributes would therefore suggest that ultrasound-mediated microbubble-enhanced gene transfer could provide an ideal means of remotely controlling gene transfer events within GAMs. With this end in mind, our group recently demonstrated that ultrasound-mediated, microbubble-enhanced gene delivery could be achieved with target cells embedded in fibrin/collagen hydrogel matrices *in vitro* (Nomikou *et al.*, 2016). In associated studies we were also able to demonstrate that should it prove necessary, an additional level of control at the transcriptional level could be incorporated into our expression plasmids to enable tight control of the therapeutic transgene expression window after delivery by ultrasound-mediated, microbubble-enhanced gene transfer (Feichtinger *et al.*, 2014).

On the basis of the above studies, we hypothesized that a MAS-based approach could be used to initiate osteogenic differentiation in a GAM for use in osteoinductive gene therapy.

Here we describe an ultrasound-responsive GAM consisting of a fibrin/collagen hydrogel matrix incorporating C2C12 cells as a surrogate osteogenic progenitor target, polymeric microbubbles, together with constitutive and inducible therapeutic plasmid DNA capable of co-expressing bone morphogenic proteins 2 and 7 (BMP2/7). We demonstrate that it can be used to enable osteogenic differentiation *in vitro* and demonstrate that it can be employed to provide enhanced ectopic bone formation in response to site-directed, exposure to externally applied ultrasound *in vivo*. The ability to non-invasively initiate osteogenic differentiation suggests this ultrasound-responsive GAM could provide a novel means of controlling gene-based therapies in regenerative medicine.

2. Materials and Methods

2.1. Plasmid DNA and cell culture

The inducible and constitutive single-vector BMP2/7 co-expression plasmids, pTetON-BMP2/7 and pVAX1-BMP2/7 have been described previously (Feichtinger *et al.* 2014). The reporter plasmid pCMV-Luc, encoding the firefly luciferase gene under the control of the CMV promoter, was supplied by PlasmidFactory GmbH & Co (Germany). C2C12 mouse myoblast precursor cells were obtained from in-house stocks and used as both an *in vitro* and a matrix-implanted *in vivo* target for gene transfer and expression in 3D matrices. The cell line was maintained in high glucose-containing tissue culture medium (Dulbecco's modified Eagle's medium; DMEM) supplemented with glutamine (GibcoBRL, UK) and 5% (v/v) fetal bovine serum (Life Technologies, UK) at 37°C in a 5% CO₂ humidified atmosphere. When required, single cell suspensions were prepared by treating cell monolayers with a 0.05% (w/v) solution of trypsin containing 0.02% (w/v) EDTA in phosphate-buffered saline (PBS). Cells were subsequently harvested and washed in Opti-MEM reduced serum medium by centrifugation prior to use.

2.2. Preparation of microbubbles

Polymeric microbubbles were prepared as described previously (McEwan et al., 2014). Microbubbles were stored as a freeze-dried preparation and prior to use were reconstituted with PBS, followed by several washes by centrifugation in order to remove the polymeric debris. After each wash microbubbles were recovered from the surface of the suspension using a pipette. The microbubble suspension was diluted in PBS when necessary.

2.3. Preparation of cell-containing 3D matrices for matrix-assisted sonoporation (MAS)

Figure 1.

3D matrices containing target cells were prepared as described previously (Nomikou *et al.*, 2016) except that a 15 μ L aliquot of polymeric microbubble suspension replaced lipid-shelled microbubbles and the pCMV-Luc plasmid was replaced with the therapeutic plasmids described above. Unless otherwise stated, each 80 μ L aliquot of matrix contained 4×10^5 cells, together with microbubbles at a concentration of 10^8 microbubbles/ml and plasmid DNA at a concentration of 80 μ g/mL (resulting in 6.4 μ g total DNA dose per construct). For matrices in the absence of microbubbles and DNA, the suspension/solution was replaced by PBS and Opti-MEM, respectively. For *in vitro* experiments, the mixture was left to gel for 10–15 s at room temperature. For *in vivo* experiments, the mixture was injected into the hind leg muscle of nude mice before gelation occurred using an insulin syringe.

2.4. MAS-mediated gene transfer & osteogenic differentiation in vitro

For *in vitro* experimentation, after each matrix had gelled, each well was treated with ultrasound, as described previously (Nomikou et al., 2016), using an SP100 sonoprotector

(Sonidel Ltd., Ireland) emitting ultrasound at a frequency of 1 MHz. The transducer had an effective radiating area of 0.8 cm². Samples were treated at a power density of 4 W/cm² (spatial average:temporal peak; SATP) using a 25% duty cycle (pulse frequency 100 Hz), for 30 s (providing an energy density of 30 J/cm² per treatment). Matrices were treated by placing the ultrasound transducer underneath the corresponding well. Contact between the multi-well plate and the transducer was mediated by ultrasound gel. Following ultrasound treatment, a 150 µL aliquot of Opti-MEM was added to each well and the plates were placed in a humidified 5% CO₂ atmosphere at 37°C for 1 h. Each matrix was then transferred to a well of a 24-well plate with 2 mL of high glucose-containing DMEM supplemented with glutamine (GibcoBRL, UK) and 5% (v/v) foetal bovine serum and plates were incubated at 37°C in a humidified 5% CO₂ atmosphere. Every 48 h, the medium in the matrix-containing wells was renewed. 2 µL of doxycycline solution (1000ng/µL) was also added to the incubation medium of the matrices containing the pTetON-BMP2/7 inducible construct, once every 48 h.

2.4.1. Bioluminescence imaging based quantification of gene transfer in vitro

Bioluminescent imaging was used to assess ultrasound-mediated gene transfer using the luciferase-encoding reporter plasmid, pCMV-Luc as described previously (Nomikou *et al.*, 2016). Bioluminescence was recorded after 20 min, using a Xenogen IVIS® Lumina imaging system supported by Living Image® software v. 2.60. Using this software, each well was marked as a region of interest (ROI) and luciferase activity was expressed as photons emitted/s from each well.

2.4.2. Alkaline phosphatase (ALP) assay for osteogenic differentiation in vitro

Alkaline phosphatase production was employed as an osteogenic differentiation marker in GAMs and its production in matrices was determined 7 days post-treatment. Each matrix was

immersed in 300 μL of a 10 mg/mL p-nitrophenyl phosphate solution in ALP buffer (0.5 M 2-amino-2-methyl-1-propanol, 2 mM magnesium chloride, pH 10.3) and incubated at 37°C for 60 minutes. The reaction was terminated by the addition of 50 μL of NaOH to a final concentration of 0.2 M in each sample. The absorbance at 405 nm was determined using a VersaMax microplate reader (Molecular Devices, USA) and the activity of ALP delivered by the non-lysed clots was expressed as nmoles of p-nitrophenol (pNP) released per minute for each clot. For subsequent histological analyses, matrices were fixed and stored in absolute ethanol.

2.4.3. Measurement of cell viability in 3D matrices

Cell viability in 3D matrices was determined using the method described previously (Nomikou *et al.*, 2016) and was based on an increase in fluorescence as a result of the cleavage of fluorescein diacetate (Fda) by esterase activity in viable cells. The fluorescence intensity of each matrix was measured using a FLUOstar Omega microplate reader (BMG Labtech, Germany), an excitation wavelength of 485 nm and an emission wavelength of 520 nm. Since this protocol was non-destructive, repeated measurement of cell viability was possible if the excess fluorescein was removed. When necessary, this was accomplished by washing twice under sterile conditions with medium (30 min/rinse) and subsequent incubation in a humidified 5% CO₂ atmosphere at 37°C until required for further analysis. Cell viability rate (CVR) is a relative term defined by $\text{CVR} = \text{F}_{\text{tn}}/\text{F}_{\text{t0}}$, where F_{tn} is the fluorescence detected at a defined time point post embedding cells in matrices and F_{t0} is the fluorescence detected immediately after embedding cells in matrices.

2.4.4. Histological analysis of matrices from in vitro studies

Von Kossa staining was used to detect calcium deposits within treated matrices. Following fixation in ethanol as described above, matrices were embedded in paraffin wax and 5 µm thick serial sections were prepared using a microtome (Leica). Positive controls for osteogenic differentiation contained 300 ng of recombinant BMP2 (Induct OS® recombinant CHO-derived human BMP2, Pfizer GmbH, Austria) per clot. The sections were then deparaffinised, hydrated in water and rinsed in several changes of distilled water. Sections were incubated in a 1% (w/v) silver nitrate solution under ultraviolet light for up to 30 minutes followed by several rinses in distilled water. Unreacted silver stain was removed by incubating the slides for 5 minutes with sodium thiosulphate followed by multiple rinses in distilled water. Sections were then counterstained with nuclear fast red for 5 minutes, rinsed in distilled water before being dehydrated in absolute ethanol, cleared in xylene and mounted in DPX. Immunohistochemical analysis of matrices for osteocalcin expression was also performed on 5 µm thick alcohol-fixed paraffin sections. Endogenous peroxidase activity was blocked using 2% (v/v) hydrogen peroxide and chymotrypsin (Sigma) enzymatic antigen retrieval was carried out by incubating sections in a 0.1% (w/v) enzyme solution (pH 7.8) for 30 minutes. Samples were incubated overnight at 4°C with mouse osteocalcin-specific primary antibody (1:100 dilution; Abcam, UK) and staining was achieved using peroxidase conjugated secondary antibody as per the manufacturer's protocol (EnVision Kit, Dako, UK). Nuclei were counter stained with haematoxylin. The stained sections were visualized using an Olympus BX50 microscope and imaged using NIS Elements BR software (Ver. 3.0).

2.5. MAS-mediated gene transfer & osteogenesis in vivo

All animals were treated humanely and in accordance with licensed procedures under the UK Animals (Scientific Procedures) Act 1986. Prior to injection of the matrix formulation and

ultrasound treatment, animals were anaesthetized by intraperitoneal injection of Hypnorm:Hypnovel. The cell-containing 3D matrices were prepared as described above (Section 2.3) and 80 μ L immediately injected into the hind leg muscle of nude mice (Hsd:Athymic Nude-Foxn1nu mice, Harlan Laboratories, UK) prior to gelation. Four minutes after injection, the area was treated with ultrasound for 60 s using an SP100 (Sonidel Ltd., Ireland) sonoprotor at a frequency of 1 MHz, a power density of 4 W/cm² (spatial average:temporal peak; SATP) and using a 50% duty cycle (pulse frequency 100 Hz). A conventional ultrasound gel was employed to ensure adequate contact between the ultrasound transducer surface and skin. Animals were sacrificed 30 days after treatment and the treated limbs were surgically recovered, fixed in 10% formalin for 48 h and subsequently stored in 70% (v/v) ethanol. In these experiments 4 limbs were treated per group and each group was treated with; (A) matrix containing cells, microbubbles and DNA in the absence of ultrasound (GAM without ultrasound); (B) matrix plus cells and microbubbles without DNA and treated with ultrasound (GAM without DNA with ultrasound); (C) matrix containing cells, microbubbles, DNA and treated with ultrasound (GAM treated with ultrasound) and (D) microbubbles and DNA in the absence of cells and treated with ultrasound.

2.5.1. Micro Computed Tomography (μ CT) analysis of ectopic bone formation

Images of target limbs were obtained using a SCANCO μ CT 50 (70 kVp 17.2 μ m, \geq 2100 HU) (SCANCO Medical, Switzerland). The measurements were performed using the SCANCO evaluation software on the μ CT. A ROI was drawn which included the entire limb but excluded the endogenous limb bones. This ROI provided a threshold intensity level of 2100 HU to identify sites of higher x-ray absorption within the limb. Each of these sites was visually inspected to ensure that (i) no bone fragments had adhered to the skin during surgical recovery of the limb and (ii) image artefacts were not being identified as ectopic bone. Bone volume

(mm³) and bone mineral density (mg hydroxyapatite per cm³) were calculated using the instrumentation operating system.

2.5.2. *Histological analysis of tissues from in vivo studies*

Fixation was performed in 4% formalin, rinsed in water and transferred to 50 and 70% alcohol. After μ CT samples were dehydrated completely by an increasing series of alcohol immersed prior to embedding into paraffin in the intermedium xylol for histological processing. Serial sections of 4 μ m were prepared using a rotatory microtome (HM 355S Microm) and dried overnight. After de-paraffinisation, sections were analysed using van Kossa staining for mineralized material according to a standard protocol using Mayer's haematoxylin as nuclear counter-stain. Positively stained areas were considered to be ectopic tissue if the location correlated with the anatomical location of granules identified in μ CT scans, if they were located in the muscle or the associated connective tissue and if no sign of long bones (e.g. growth plate) was evident.

2.6. *Statistical analysis*

Statistical analysis of significance for *in vitro* data was conducted using ANOVA and normally distributed data groups were compared with the Tukey multiple comparison test (MCT), using GraphPad Prism 4.0. Unless stated otherwise, $p < 0.05$ was considered to indicate statistical significance. *In vivo* bone volumes and bone mineral densities were assumed to be normally distributed and therefore analysed by ANOVA and Newman Keuls post-test, accepting significance at $p < 0.05$.

3. Results

3.1. MAS-mediated gene transfer & osteogenic differentiation in vitro

3.1.1. Bioluminescence imaging based quantification of gene transfer in vitro

Prior to embarking on the osteogenic differentiation studies it was decided to confirm that the use of increased concentrations of the polymeric microbubbles together with increased concentrations of target cells within matrices would provide ultrasound-mediated gene transfer. To this end the pCMV-Luc plasmid encoding the luciferase reporter gene was used in matrices pre-loaded with target cells and microbubbles. The data (Figure 2A) demonstrated that, in the absence of ultrasound treatment, luciferase expression in matrices was low, whereas following treatment with ultrasound, expression of the reporter gene increased over 25-fold. The data demonstrated that ultrasound-mediated gene transfer occurred in these new matrices using the polymeric microbubbles and using higher concentrations of target cells and microbubbles than those used previously (Nomikou *et al.*, 2016). When luciferase expression was examined at day 7 post application of ultrasound, it was noted that the level of gene expression had decreased (Figure 2A) and this confirmed that expression of the transgene was transient using this system.

Figure 2.

3.1.2. Measurement of cell viability in 3D matrices

Since higher concentrations of target cells and microbubbles were employed in matrices in the current studies and in the presence of an ultrasonic field this could potentially have a deleterious effect on target cells, it was also decided to examine the effect of ultrasound treatment on cell

viability within matrices. Matrices were treated with ultrasound conditions used to effect gene transfer and cell viability was determined at 24 h, 48 h and 120 h after treatment. Cell viability in control matrices that had not been treated with ultrasound was also determined for comparative purposes. Results shown in Figure 2B demonstrate that C2C12 cells remained viable and proliferated over time, even at the high cell and microbubble concentrations used and these data served to further validate the use of the polymeric microbubbles in matrices.

3.1.3. MAS-mediated induction of osteogenic differentiation in vitro

3.1.3.1. Alkaline phosphatase activity

Having demonstrated that ultrasound could be used to facilitate gene transfer and expression in 3D matrices without any negative impact on cell viability using high cell numbers with the new polymeric microbubbles, it was decided to use the approach to enable gene transfer of therapeutic plasmids co-expressing BMP2 and BMP7 into C2C12 cells and determine whether or not this would result in osteogenic differentiation. To this end, the effect of microbubbles and ultrasound on the delivery of the BMP2/7-co-expressing plasmid constructs (Feichtinger *et al.*, 2014) (either pTetON-BMP2/7 or pVAX1-BMP2/7) and resultant osteogenic differentiation was examined in 3D matrices containing C2C12 cells. Where the inducible pTetON-BMP2/7 plasmid was used, the inducer doxycycline was added to the system. Ultrasound was used at a power density of 4 W/cm², using a 25% duty cycle and samples were treated for 30s. Alkaline phosphatase was used as an endpoint for osteogenic differentiation and when it was determined in the 3D matrices 7 days post-treatment the results shown in Figure 2C and D were obtained. The data clearly demonstrate that for both constitutive expression plasmid pVAX-BMP2/7-containing matrices (Figure 2C) and the doxycycline inducible expression plasmid (pTetON-BMP2/7)-containing matrices (Figure 2D) with

incorporated microbubbles and treated with ultrasound (MAS treated), alkaline phosphatase activity was significantly higher than the corresponding control systems. In particular, for the pVAX-BMP2/7 system, in matrices that were not exposed to ultrasound and in matrices treated with ultrasound in the absence of microbubbles, alkaline phosphatase activity was 2.4- and 2.2-fold lower, respectively, than the MAS-treated samples. For the pTetON-BMP2/7 system, in matrices that were not irradiated with ultrasound and in matrices treated with ultrasound in the absence of microbubbles, alkaline phosphatase activity was 2.7- and 2.4-fold lower, respectively, than the MAS-treated samples. In addition, when matrices containing the pTetON-BMP2/7 inducible plasmid in the absence of the inducer doxycycline were treated with MAS, alkaline phosphatase activity was similarly low. The latter result confirms that the increase in alkaline phosphatase activity detected in MAS-treated samples resulted from MAS-specific gene transfer events. It also demonstrates tight control of therapeutic transgene expression at the transcriptional level by doxycycline after MAS, where its addition to matrices led to a 1.5-fold increase in alkaline phosphatase activity over that obtained with the system employing the constitutive plasmid (pVAX1-BMP2/7) (Figure 2C, D).

3.1.3.2. Histological examination of matrices from in vitro studies

In addition to using the measurement of alkaline phosphatase expression at day 7 as a marker of osteogenic differentiation, the latter was confirmed by histological analysis for bone mineralisation and osteocalcin expression at day 14 post treatment. To this end von Kossa staining for mineralisation and immuno-histochemical staining for osteocalcin were carried out on matrices harvested at day 14 post ultrasound treatment. Positive control matrices were generated by incorporation of 300 ng of recombinant BMP2 growth factor into C2C12-containing matrices. In qualitatively examining areas of interest within stained sections of the positive control, successful induction of osteogenic differentiation was suggested by the

presence of strongly positive mineral deposition (black specks) and more intense osteocalcin staining present (Figure 3-A1). Cells in MAS treated constructs without BMP2/7 co-expression plasmids or recombinant BMP2 treatment did not show mineral deposits or osteocalcin staining (Figure 3-A2). Qualitatively constructs containing the constitutive co-expression system pVAX-BMP2/7 and treated with MAS provided the most intense staining for mineralisation and osteocalcin (Figure 3-B1) when compared with control samples in the absence of ultrasound or treated with ultrasound in the absence of microbubbles (Figure 3-B2, B3 respectively). The highest overall staining was observed in MAS treated matrices containing the inducible pTetON-BMP2/7 system in the presence of doxycycline (Figure 3-C1). Staining of the doxycycline induced control matrices in the absence of ultrasound (Figure 3-C3) or treated with ultrasound in the absence of microbubbles (Figure 3-C4) suggested low-level differentiation when compared with MAS treated samples. For clarity, higher resolution images of selected sections are provided in Figure 3 D, E and F.

Figure 3.

3. 2. MAS-mediated gene transfer & osteogenesis in vivo

Since the above findings suggested that ultrasound could be employed to facilitate osteogenic differentiation in a GAM harbouring a suitable recipient progenitor cell model *in vitro*, it was felt that it could provide an alternative to *ex vivo* gene-based therapies (Balmayor and van Griensven, 2015) for bone repair. Therefore, in subsequent experiments the liquid GAM was injected into the hindlimb muscle of recipient mice before it had gelled and osteogenesis was probed using μ CT and histological analyses.

3.2.1. Micro Computed Tomography (μ CT) analysis of ectopic bone formation

The data obtained from μ CT analysis are shown in Figure 4 and demonstrate positive ectopic bone formation in: 4 out of 4 (100%) limbs in group treated with the complete GAM an ultrasound (Figure 4C); 2 out of 4 (50%) limbs in the passive, GAM-mediated gene delivery control group without ultrasound treatment (Figure 4A) and 3 out of 4 (75%) limbs in the ultrasound treated, standard sonoporation control group without exogenous cells (Figure 4D). When the matrices including cells were delivered to control limbs without the plasmid, only one limb was found to contain minute amounts of ectopic bone (Figure 4 B). Analysis of total bone volumes achieved per treatment site/animal revealed that MAS-mediated osteogenic gene delivery leads to a significant increase of formed bone volumes (Figure 4E) compared to all other groups (5.7-fold increase compared to passive, GAM-mediated delivery and 16.44-fold compared to standard sonoporation under current conditions), clearly demonstrating the therapeutic advantage of the novel approach over current non-viral gene delivery methods. Bone mineral densities (BMD) of new ectopic bone ranged from 750 to 1040 mg hydroxyapatite/cm³ of analysed bone volume with no significant differences amongst groups examined.

Figure 4:

3.2.2. Histological analysis of tissues from in vivo studies

Histological examination of μ CT positive MAS-treated samples confirmed mineralised nodules at ectopic sites in muscles by von Kossa staining (Figure 5A-C). Morphologically, the MAS-induced ectopic intramuscular bone structures exhibited a complex architecture including compact bone, structures with a bone marrow cavity with cells appearing like haematopoietic bone marrow and in some cases, even cartilage-like formations (Figure 5 B).

Figure 5.

4. Discussion

4.1. MAS-mediated gene transfer & osteogenic differentiation *in vitro*

The efficacy of ultrasound in combination with microbubbles for *in situ* gene transfer in 3D matrices has been recently demonstrated by our group *in vitro* (Nomikou *et al.*, 2016). In that study, the myoblast precursor cell line C2C12 was embedded in fibrin/collagen-based matrices containing ultrasound-responsive lipid-shelled microbubbles and a luciferase-expressing plasmid (pCMV-Luc). Since the ultrasound-responsive fibrin/collagen-based matrices employed in those studies could be formulated as a liquid, combined with suitable target cells and subsequently administered by injection before gelation, it was felt, that it presented an ideal tool for use in minimally-invasive tissue regenerative GAM-based approaches. However, if the system was to be employed for such purposes it would be necessary to demonstrate that ultrasound-stimulated gene transfer within matrices could provide levels of gene expression by embedded target cells that would be sufficient to induce differentiation of those cells within the administered hydrogel. In realising such an outcome, it was decided to modify the original matrix by incorporating more stable polymeric microbubbles that would persist within the matrix for longer periods of time (McEwan *et al.*, 2014). In our previous study we used cationic microbubbles to maximise interaction between nucleic acid, microbubbles and target cells so that this would, in turn, enhance ultrasound-mediated gene transfer (Nomikou *et al.*, 2016). Therefore, to enhance interaction between the polymeric microbubbles and the target cells within matrices, it was decided to use both at concentrations that were higher than those used in our previous study (Nomikou *et al.*, 2016) since this approach was shown to provide the same benefit afforded using cationic microbubbles (Nomikou *et al.*, 2012). The results

obtained served to validate our use of the more stable polymeric microbubbles in the GAM for MAS-based gene transfer. Apart from clearly demonstrating an improvement of gene transfer by MAS without impacting negatively on target cell viability within matrices, the data in Figure 2 also demonstrate that gene expression in the ultrasound-treated system dropped almost 7-fold after 7 days. Demonstrating transient expression of the transgene could prove very useful from a temporal control perspective in bone regeneration because it has been shown that a number of genes are transiently expressed during osteogenic differentiation and bone regeneration (Javed *et al.*, 2010). It could also be advantageous from a safety perspective because it could preclude many of the adverse effects associated with high therapeutic levels of BMP (Hustedt and Blizzard, 2014).

Cell differentiation studies clearly demonstrated that MAS-mediated delivery of both the constitutive and inducible BMP2/7 expression systems led to a significant increase in osteogenesis as evidenced by quantitative ALP data and qualitative histological evaluation when compared with controls. Controls exhibited low-level differentiation as indicated by the expression of ALP without ultrasound-stimulation, which may have resulted from passive gene delivery. In the current study we demonstrate a 2.7-fold increase in ALP following treatment with ultrasound. Using lipofection to transfer separate plasmids encoding BMP2 and BMP7 into C2C12 cells, Kawai *et al* (2006) demonstrated a 7-fold increase in ALP. However, in the latter case the target cells were not embedded in a matrix. In overall terms, the alkaline phosphatase data, taken together with the histological analyses clearly demonstrate that MAS treatment *in vitro* facilitates stimulus-responsive gene transfer into the GAM-embedded target cell population (C2C12 cells) that is sufficient to drive osteogenic differentiation. The data essentially demonstrate that it is possible to control gene transfer-dependent osteogenic differentiation within GAMs *in vitro* using an external stimulus. The data obtained with the TetON system also suggest that additional control of transgene expression and subsequent

osteogenic differentiation can be incorporated into the novel GAM by judiciously manipulating control of expression of therapeutic nucleic acid constructs that would respond to inducers *in vivo* at a molecular genetic level as shown in previous work (Feichtinger et al., 2014a).

4. 2. MAS-mediated gene transfer & osteogenesis *in vivo*

In order to confirm the therapeutic potential offered by our approach it was decided to examine its ability to generate ectopic bone in murine muscle *in vivo*. The pVAX-BMP2/7 plasmid was used here since it would be more appropriate for future clinical translation and would not be reliant on the addition of an exogenous inducer. Use of this plasmid would also preclude any inducer-mediated effects so that osteoinduction would be the sole result of therapeutic gene transfer following the exposure to ultrasound. One of the major advantages of this GAM is that it is formulated as a liquid to enable injection into a chosen site and the fibrin gelling time may be adjusted to facilitate gelling directly post injection prior to activation. Being able to accomplish this offers the advantage of retaining the therapeutic entity (osteogenic progenitor cells and therapeutic nucleic acids) at the desired site thereby minimising off-target bone generation. It could also potentially allow the intraoperative preparation of a therapeutic gene therapy formulation (Evans and Hurd, 2015) if primary cell sources such as bone marrow or liposuction aspirates were available. In contrast to the *in vitro* prepared GAM of this study and other examples of so-called ‘gene plugs’ (Pascher *et al.*, 2004), where gene transfer is carried out extracorporeally and the matrix is then press-fit into the defect area, the current approach could facilitate moulding of the injectable liquid matrix into a defect and allow post implantation gene transfer events. Essentially the GAM could be compatible with either *ex vivo* gene transfer and subsequent surgical implantation as indicated by the *in vitro* data above or with surgical implantation followed by *in vivo* gene transfer. The *in vivo* ectopic bone formation data obtained above suggest that this GAM could play a role in approaches involving

the latter. The data demonstrated that the highest frequency of bone formation (100%) was delivered with MAS and this is in line with previous studies showing that sonoporation can significantly increase the frequency of successful gene delivery and associated bone formation *in vivo* (Feichtinger *et al.*, 2014). The novel outcome of the current study regarding the significantly (5.4- to 16.4-fold) increased yields of bone volumes attainable with MAS (Figure 4) compared to all other standard treatment modalities (passive GAM and sonoporation) is furthermore superior to those from previous studies by us and other groups in which multiple rounds of sonoporation and higher DNA doses were necessary for tissue formation (Feichtinger *et al.*, 2014; Osawa *et al.*, 2009). In our previous studies using a cell and matrix-free sonoporation-based approach it was necessary to use 100 µg of DNA and an ultrasound energy density of 90-600 J/cm² whereas here we used 6.5 µg of DNA and an ultrasound energy density of 30 J/cm² (Feichtinger *et al.*, 2014). Thus, the current study provided bone formation in all limbs treated with a single MAS treatment and used much lower overall DNA and ultrasound doses. Being able to employ lower quantities of therapeutic nucleic acid could have important benefits in terms of precluding non-specific gene transfer events that could lead to off-target bone formation.

It should also be noted that BMD values observed for ectopic structures were higher than those observed in previous studies using standard sonoporation alone (250 mg HA/cm³ at 28 days) (Feichtinger *et al.*, 2014) and ranged between reported values for cancellous (250-650 mg HA/cm³) and cortical bone (1050-1250 mg HA/cm³) in mice (Entezari *et al.*, 2012). Although the formation of complex ectopic bone structures with a stem cell niche has previously been demonstrated in multiple *in vivo* gene therapy studies including our own using BMPs as therapeutic genes (Osawa *et al.*, 2010), the appearance of a cartilage-bone interface as observed in one sample in this study is interesting (Figure 5B). There are also indications in the literature that C2C12 cells specifically respond to certain BMP signalling cues which might

be present in the current setup and thus, the chosen therapeutic gene combination and administered target cell type might be the determinant of the observed cartilage formation in the present study. It has been shown that C2C12 cells can respond to BMP4 and differentiate down the chondrogenic lineage and can form ectopic bone and cartilage *in vivo* (Li et al., 2005). Interestingly, the BMP2/7 expression strategy used in the current study has been shown by others to specifically induce expression of BMP4 after BMP2/7 gene transfer *in vivo* (Kawai et al., 2006). Therefore, it might be possible that BMP2/7 expression resulted in endogenous BMP4 expression, which in turn can induce chondrogenic differentiation of C2C12 cells *in vivo* and result in the observed morphologically complex ectopic structures (Figure 5B). Although more appropriate staining procedures could be employed to confirm our observations relating to the presence of cartilage and bone marrow-like structures, this could represent a specific effect linked to the responsiveness of the exogenously-added cells in the current study and might explain the difference between previous *in vivo* gene therapy studies without cells in the GAM, indicating an additional level of control of tissue formation in the current setup by incorporation of certain specific progenitor cells into the GAM for MAS.

The MAS approach devised in this study could be developed for translation to human patients using clinically relevant mesenchymal stem cell sources (Alhadlaq,2004) such as adipose derived stem cells, bone marrow derived mesenchymal stem cells or any other source of autologous adult, expression capable somatic cells that can be harvested intra-operatively in a one-step intervention (Gafni et al., 2004) to enable straightforward translation. As the proposed strategy is reliant on the *in situ* expression of sufficient amounts of BMP, which can also act as a chemotactic cue for endogenous stem cells to home to the defect (Zhang et al., 2014), the abundance, ease of harvesting and receptiveness to transgene delivery and expression of any target cell population is more important for the approach than the differentiation capabilities of the cells themselves, which are mainly required to act as drug

production/delivery vehicles in the current approach. Nevertheless, if expression capable and differentiation capable mesenchymal stem cells are to be used in any future translation of the MAS approach, therapeutic efficacy might be improved by combining both synergistic properties of the target cell population, enhancing therapeutic efficacy and potentially compensating for limited transfection efficacy. The next stages in the preclinical development of the therapeutic MAS-based approach presented in the current work would therefore involve incorporation of a clinically relevant somatic cell source together with evaluation of the therapy in an appropriate preclinical orthotopic bone regeneration model. Subsequent studies would also include an assessment of the quality of the resulting bone formed within the chosen model defect to allow for mechanical testing.

5. Acknowledgements

This work has been funded by the European EUROSTARS project UGen (E!5650) and partially funded by the European ANGIOSCAFF project (NMP-2007-2.3-1). The authors would like to acknowledge Mrs. Jackie Hudson for her assistance with the *in vitro* von Kossa stainings and Dr. Ara Hacobian for kindly providing the MAS scheme depicted in Figure 1.

6. Conflict of Interest

The authors declare that they have no conflicts of interest.

7. References:

Alhadlaq, J.M. 2004, Mesenchymal Stem Cells: Isolation and Therapeutics. *Stem Cells and Development*, 2004. **13**: 436-448.

Balmayor ER, van Griensven M. 2015, Gene therapy for bone engineering. *Front Bioeng Biotechnol*, **3**:9, doi: [10.3389/fbioe.2015.00009](https://doi.org/10.3389/fbioe.2015.00009)

Bonadio J. 2000, Tissue engineering via local gene delivery: Update and future prospects for enhancing the technology. *Adv Drug Deliv Rev*, **44**:185-194.

Entezari V, Vartanians V, Zurakowski D, Patel N, Fajardo RJ, Muller R, Snyder BD, Nazarian A. 2012, Further improvements on the factors affecting bone mineral density measured by quantitative micro-computed tomography. *Bone* **50**:611-618.

Escoffre JM, Zeghimi A, Novell A, Bouakaz A. 2013, In-vivo gene delivery by sonoporation: recent progress and prospects. *Current Gene Ther*, **13**:2-14.

Evans CH, Huard J. 2015, Gene therapy approaches to regenerating the musculoskeletal system. *Nat Rev Rheumatol*, **11**:234-242.

Feichtinger GA, Hacobian A, Hofmann AT, Wassermann K, Zimmermann A, van Griensven M, Redl H. 2014a, Constitutive and inducible co-expression systems for non-viral osteoinductive gene therapy. *Eur Cell Mater*, **27**:166-184; discussion 184.

Feichtinger GA, Hofmann AT, Slezak P, Schuetzenberger S, Kaipel M, Schwartz E, Neef A, Nomikou N, Nau T, van Griensven M, McHale AP, Redl H. 2014. Sonoporation increases therapeutic efficacy of inducible and constitutive BMP2/7 in vivo gene delivery. *Hum Gene Ther Methods*, **25**:57-71.

Gafni Y, G.T., Liebergal GT, Pelled G, Gazit Z, Gazit D. 2004, Stem cells as vehicles for orthopaedic gene therapy. *Gene Therapy*. **11**: 417-426.

Gonzalez AM, Berry M, Greenlees L, Logan A, Baird A. 2006, Matrix-mediated gene transfer to brain cortex and dorsal root ganglion neurones by retrograde axonal transport after dorsal column lesion. *J Gene Med*, **8**: 901-909.

Hustedt JW, Blizzard DJ. 2014, The controversy surrounding bone morphogenetic proteins in the spine: a review of current research. *Yale J Biol Med*, **87**:549-561.

- Jafari M, Soltani M, Naahidi S, Karunaratne DN, Chen P. 2012, Nonviral approach for targeted nucleic acid delivery. *Curr Med Chem*, **19**:197-208.
- Javed A, Chen H, Ghorri FY. 2010, Genetic and transcriptional control of bone formation. *Oral Maxillofac Surg Clin North Am*, **22**:283-293.
- Kawai M, Bessho K, Maruyama H, Miyazaki J, Yamamoto T. 2006, Simultaneous gene transfer of bone morphogenetic protein (BMP) -2 and BMP-7 by in vivo electroporation induces rapid bone formation and BMP-4 expression. *BMC Musculoskelet Disord*, **7**:62, doi:10.1186/1471-2474-7-62
- Kayabasi GK, Aydin RS, Gumusderelioglu M. 2013, *In vitro* chondrogenesis by BMP6 gene therapy. *J Biomed Mater Res A*, **101**:1353-61.
- Kimelman-Bleich N, Pelled G, Zilberman Y, Kallai I, Mizrahi O, Tawackoli W, Gazit Z, Gazit D. 2011, *Mol Ther*, **19**, 53-59.
- Lammertink BH, Bos C, Deckers R, Storm G, Moonen CT, Escoffre JM. 2015, Sonochemotherapy: From bench to bedside. *Front Pharmacol*, **6**:138, doi: 10.3389/fphar.2015.00138
- Li G, Peng H, Corsi K, Usas A, Olshanski A, Huard J. 2005, Differential effect of BMP4 on NIH/3T3 and C2C12 cells: implications for endochondral bone formation. *J Bone Miner Res*, **20**:1611-1623.
- Lu CH, Chang YH, Lin SY, Li KC, Hu YC. 2013, Recent progresses in gene delivery-based bone tissue engineering. *Biotechnol Adv*, **31**:1695-706.
- McEwan C, Fowley C, Nomikou N, McCaughan B, McHale AP, Callan JF. 2014, Polymeric microbubbles as delivery vehicles for sensitizers in sonodynamic therapy. *Langmuir*, **30**:14926-14930.

Michlits W, Mittermayr R, Schafer R, Redl H, Aharinejad S. 2007, Fibrin-embedded administration of VEGF plasmid enhances skin flap survival. *Wound Repair Regen*, **15**:360-367.

Nomikou N, Feichtinger GA, Redl H, McHale AP. 2016, Ultrasound-mediated gene transfer (sonoporation) in fibrin-based matrices: potential for use in tissue regeneration. *J Tissue Eng Regen Med*, **10**:29-39.

Nomikou N, Tiwari P, Trehan T, Gulati K, McHale AP. 2012, Studies on neutral, cationic and biotinylated cationic microbubbles in enhancing ultrasound-mediated gene delivery in vitro and in vivo. *Acta Biomater*, **8**:1273-1280.

Osawa K, Okubo Y, Nakao K, Koyama N, Bessho K. 2009, Osteoinduction by microbubble-enhanced transcutaneous sonoporation of human bone morphogenetic protein-2. *J Gene Med*, **11**:633-641.

Osawa K, Okubo Y, Nakao K, Koyama N, Bessho K. 2010, Osteoinduction by repeat plasmid injection of human bone morphogenetic protein-2. *J Gene Med*, **12**:937-44.

Pascher A, Palmer GD, Steinert A, Oligino T, Gouze E, Gouze JN, Betz O, Spector M, Robbins PD, Evans CH, Ghivizzani SC. 2004, Gene delivery to cartilage defects using coagulated bone marrow aspirate. *Gene Ther*, **11**:133-141.

Peterson CY, Shaterian A, Borboa AK, Gonzalez AM, Potenza BM, Coimbra R, Eliceiri BP, Baird A. 2009, The noninvasive, quantitative, in vivo assessment of adenoviral-mediated gene delivery in skin wound biomaterials. *Biomaterials*, **30**:6788-6793.

Ramamoorth M, Narvekar A. 2015, Non viral vectors in gene therapy- an overview. *J Clin Diagn Res*, **9**:GE01-6.

Schillinger U, Wexel G, Hacker C, Kullmer M, Koch C, Gerg M, Vogt S, Ueblacker P, Tischer T, Hensler D, Wilisch J, Ainer J, Walch A, Stemberger A, Plank C, 2008, A fibrin glue composition as carrier for nucleic acid vectors. *Pharm Res*, **25**:2946-2962.

Tierney EG, Duffy GP, Cryan SA, Curtin CM, O'Brien FJ. 2013, Non-viral gene-activated matrices: next generation constructs for bone repair. *Organogenesis*, **9**:22-8.

Wang W, Li W, Ma N, Steinhoff G. 2013, Non-viral gene delivery methods. *Curr Pharm Biotechnol*, 14:46-60.

Wang X, Helary C, Coradin T. 2015, Local and sustained gene delivery in silica-collagen nanocomposites. *ACS Appl. Mater. Interfaces*, **7**:2503-2511.

Yin H, Kanasty RL, Eltoukhy AA, Vegas AJ, Dorkin JR, Anderson DG. 2014, Non-viral vectors for gene-based therapy. *Nat Rev Genet*, **15**:541-55.

Zhang, W., C. Zhu, Y. Wu, D. Ye, S. Wang, D. Zou, X. Zhang, D.L. Kaplan, and X. Jiang. 2014. VEGF and BMP-2 promote bone regeneration by facilitating bone marrow stem cell homing and differentiation. *Eur Cell Mater*. **27**:1-11.

Figure Legends

Figure 1

Schematic representation of the matrix-assisted sonoporation (MAS) approach together with a light micrograph showing the gene activated matrix (GAM) components. Scale bar in right hand image represents 50µm.

Figure 2

Ultrasound-mediated gene transfer and differentiation *in vitro*. A. Luciferase expression (bioluminescence) by C2C12 embedded in the GAM and in the presence (+US) or absence (-US) of ultrasound on day 1 and day 7 post-treatment where n=3, and error bars represent + SEM. B. Viability of C2C12 cells embedded in the GAM in the presence (+US) and absence (-US) at 24, 48 and 120 h post-treatment where n=3 and error bars represent + SEM and *: p<0.05. Alkaline phosphatase activity in GAMs containing the constitutive plasmid pVAX1-BMP2/7 (C) and inducible plasmid pTetON-BMP2/7 (D) 7 days post-treatment; in the absence of ultrasound and presence of microbubbles (No US/MB); in the presence of ultrasound and absence of microbubbles (US/No MBs); with the complete matrix-assisted sonoporation protocol (MAS); in the absence of the inducer doxycycline (MAS/No Dox) and with MAS in the presence of doxycycline (MAS with Dox). In all cases except for No US/MB (n=2) n = 3 and error bars represent + SEM (*: p<0.05, **: p<0.01).

Figure 3

Histological staining of GAMs treated *in vitro*. Sections were stained using von Kossa (upper panels A – C with cellular counterstain in red and mineralisation in black) and osteocalcin immunochemical staining (Lower panels A – C with cellular counterstain in blue and osteocalcin staining in brown). Row A shows sections of the positive control consisting of GAMs incorporating 300 ng BMP2 per construct (A1) and those of the negative control (A2) in the absence of therapeutic plasmid DNA or growth factor. Row B shows sections from GAMs containing the constitutive plasmid, pVAX-BMP2/7 treated with MAS (B1), GAMs in the absence of ultrasound (B2) and ultrasound treatment of the GAM without microbubbles (B3). Row C shows sections from GAMs containing the inducible plasmid pTetON-BMP-2/7 treated with MAS in the presence of doxycycline (C1), GAMs treated with MAS in the absence of doxycycline (C2), GAMs treated with doxycycline without ultrasound (C3) and GAMs treated with doxycycline and ultrasound in the absence of microbubbles. Scale bars represent 100 µm. High resolution images of von Kossa- (left panel) and osteocalcin-stained (right panel) sections from GAMs treated with 300ng recombinant human BMP2 (D), GAMs containing the constitutive plasmid, pVAX-BMP2/7 and treated with MAS (E) and GAMs containing the inducible plasmid pTetON-BMP2/7 treated with MAS in the presence of the inducer doxycycline (F). Arrows highlight mineralisation positive and osteocalcin positive areas. Scale bars represent 100 µm

Figure 4

Micro-computed tomography (μ CT) scans and analysis of ectopic bone generated in vivo. (A) Images of limbs treated with the GAM without ultrasound. (B) Images of limbs treated with the GAM without DNA and with ultrasound. (C) Images of limbs treated with the complete GAM and ultrasound. (D) Images of limbs treated with microbubbles, DNA and ultrasound in the absence of the cells. Ectopic bone structures are highlighted with red circles and scale bars represent 5 mm. Bone volume analysis in mm^3 (E) represented as scatter plots where error bars represent the mean \pm SEM. * $p < 0.05$ and data were grouped to represent A, B, C and D in accordance with the μ CT images above.

Figure 5

Histological analysis of sections from ectopic bone structures in limbs following MAS treatment and stained with von Kossa (black/brown) for mineralisation and nuclear counter staining using Meyer's haematoxylin (blue). A: Ectopic bone structure showing bone marrow (*BM), bone (*B) and cartilage phase (*C) in surrounding muscle tissue (*M). Scale bar represent $200\mu\text{m}$. B: Detail of tissue interface structure found in ectopic bone structure from (A), cartilage tissue including chondrocytes in lacunae (*C) is clearly seen interfacing with a subchondral bone phase (*B) and this osteochondral phase is covering a haematopoietic bone marrow phase (*BM) with visible erythrocytes. Scale bar represent $100\mu\text{m}$. C: Ectopic bone structure showing bone marrow (*BM), bone (*B) and cartilage phase (*C) in surrounding muscle tissue (*M). Scale bar represent $100\mu\text{m}$.

Figure 1

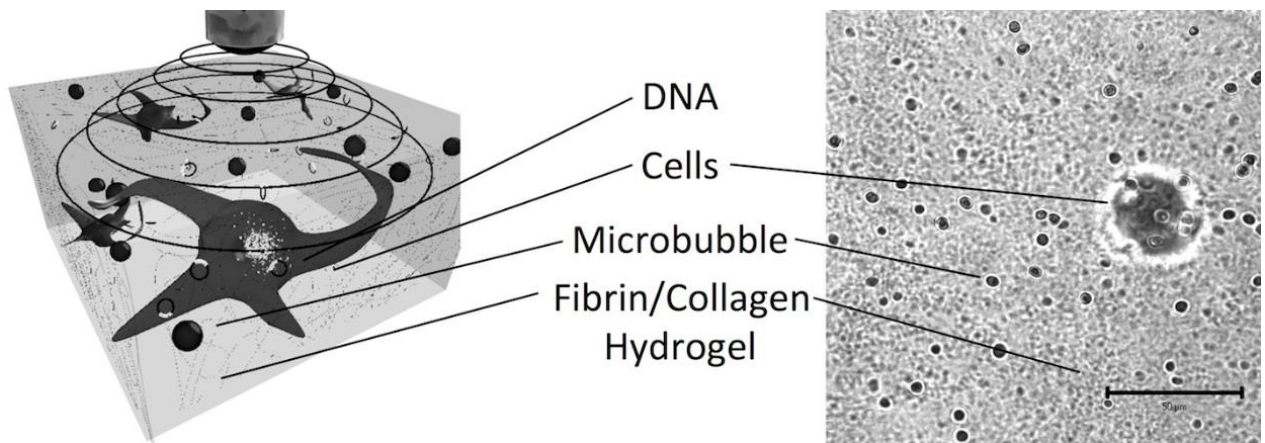


Figure 2

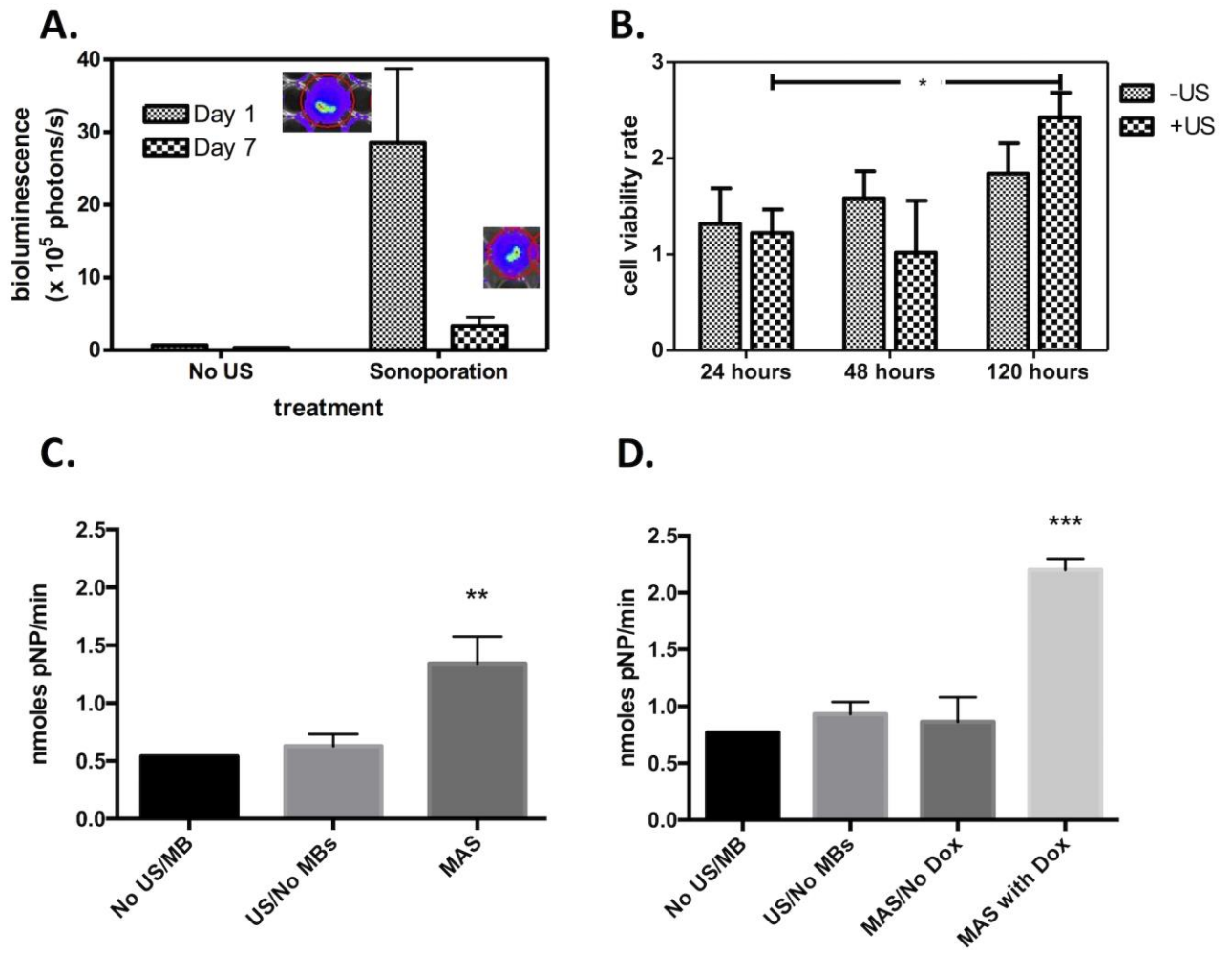


Figure 3

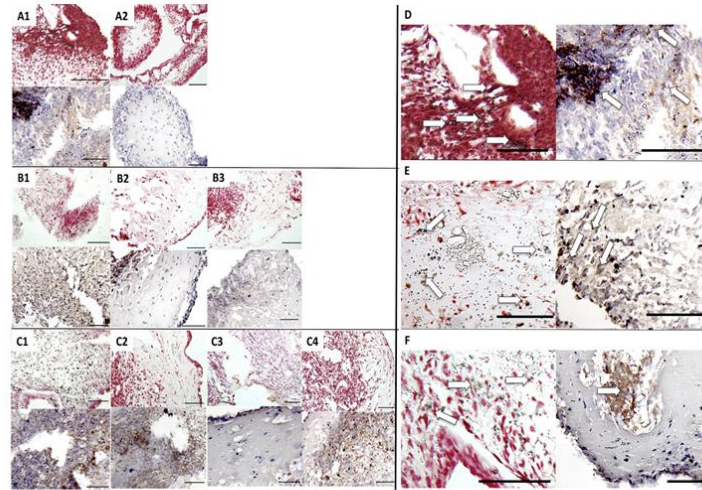
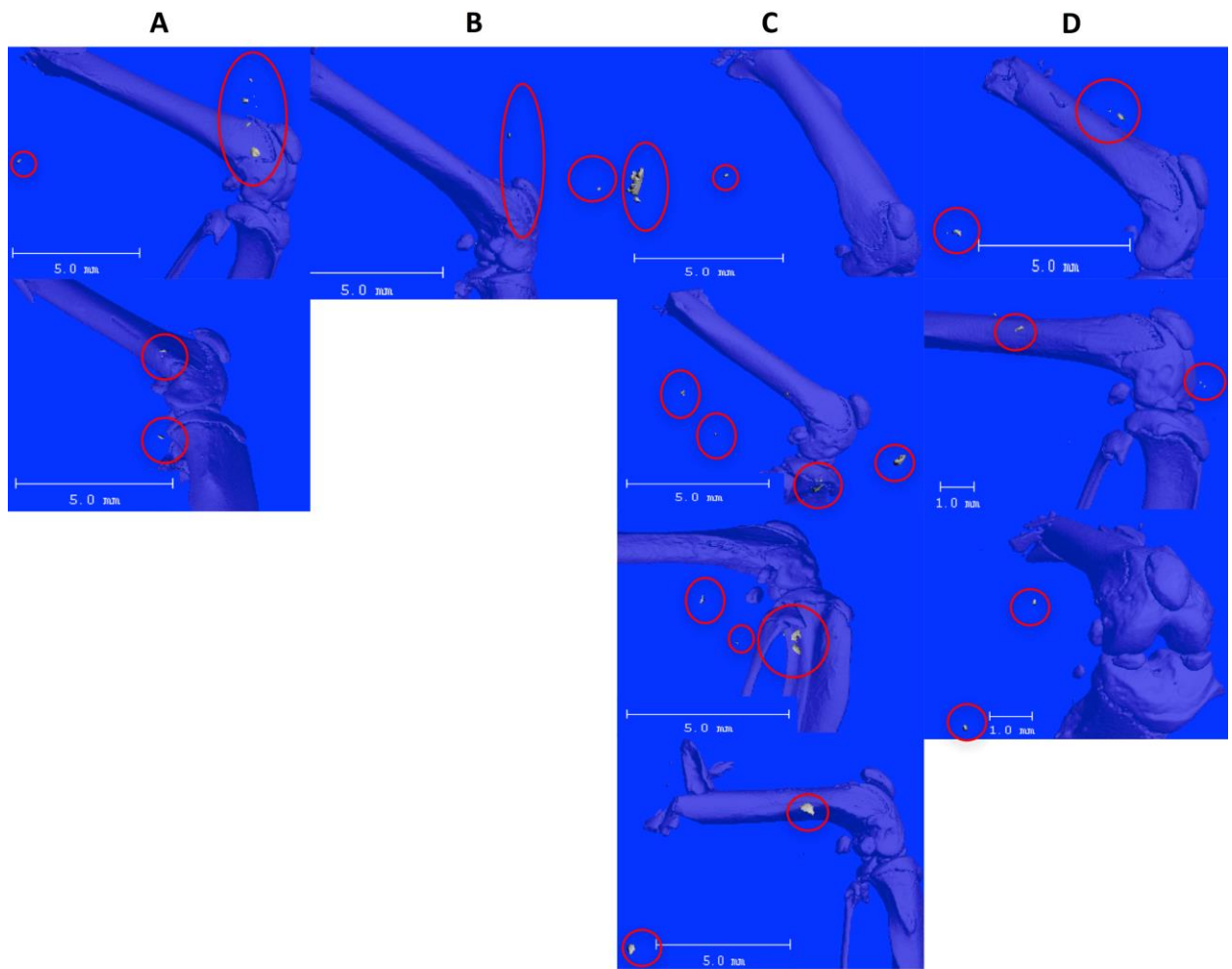


Figure 4



E. Bone volumes

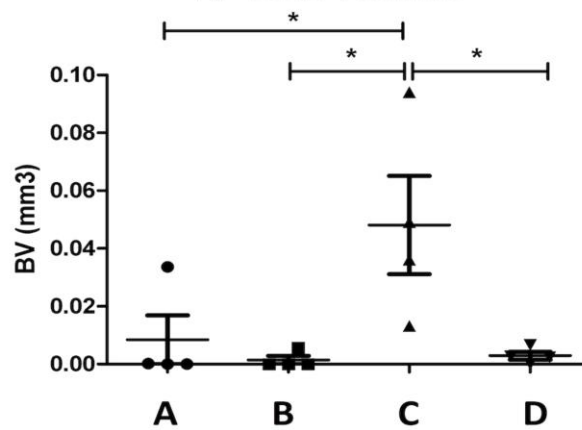


Figure 5

